Food Chemistry: X 24 (2024) 101975

Contents lists available at ScienceDirect

Food Chemistry: X

journal homepage: www.sciencedirect.com/journal/food-chemistry-x

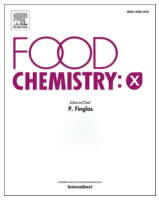

Effect of γ-irradiation combined with enzymatic modification on the physicochemical properties of defatted rice bran dietary fiber

Xuyao Wei [a,1], Caixia Jiang [a,b,1], Xiaolan Liu [c,**], Handong Liu [a], Juntong Wang [a,d], Xiqun Zheng [a,d,*], Zhi Zhang [e], Hao Hu [e]

[a] College of Food, Heilongjiang Bayi Agricultural University, Daqing 163319, China
[b] National Coarse Cereals Engineering Research Center, Heilongjiang Bayi Agricultural University, Daqing 163319, China
[c] College of Food and Biological Engineering, Qiqihar University, Qiqihar 161006, China
[d] Engineering Research Centre of the Ministry of Education for the Processing and Utilisation of Grain By-products, Daqing 163319, China
[e] Heilongjiang Beidahuang Rice Industry Group Co., Ltd, Harbin 150090, China

ARTICLE INFO

Keywords:
Rice bran
Dietary fiber
Microstructure
Physicochemical properties
Multivariate analysis

ABSTRACT

This study comprehensively examines how combining γ-irradiation and enzymatic modification influences the microstructure and physicochemical properties of dietary fiber (DF) obtained from defatted rice bran. The resulting yields of soluble dietary fiber (SDF) and insoluble dietary fiber (IDF) were measured at 13.38 ± 0.40 g/100 g and 52.19 ± 0.97 g/100 g, respectively. The modifications led to a diminish in particle size, an increase in specific surface area, and an improvement in water-holding capacity, oil-holding capacity, swelling capacity, glucose adsorption capacity, and cholesterol adsorption capacity. Furthermore, the modified DF exhibited enhanced anti-digestive properties and probiotic activity. Cluster and principal component analysis results revealed that the modified SDF exhibited superior functional properties. Correlation analysis indicated a noticeable relationship between the monosaccharide composition of DF and its functional characteristics. These findings suggest that γ-irradiation combined with enzymatic modification represents a viable approach for enhancing the quality of rice bran DF.

1. Introduction

Rice is the primary food source for a large portion of the worldwide population, particularly in Asia, South America, and Africa (Tian et al., 2024). The global annual production of rice is approximately 500 million tonnes, with China accounting for 213 million tonnes *per annum* (Park et al., 2017). Rice bran is generated during the processing of rice, making up about 5 % to 7 % of the overall mass of the rice (Wu et al., 2020). Rice bran, in addition to vitamins, minerals, and other nutrients, also contains abundant dietary fiber (DF) (Chen, Qiao, et al., 2023). Rice bran has been identified as a lesser-used natural resource by the United Nations Industrial Development Organization. The majority of rice bran is employed in the production of animal feed, resulting in the loss of valuable resources. Rice bran is abundant in DF and is increasingly recognized for its distinctive biological activity and valuable nutritional value. For the past few years, the demand for rice bran has expanded, driven by the rising emphasis on healthy diets and lifestyles (Ren et al., 2021). Rice bran is gradually being acknowledged as a dietary fiber supplement that contributes positively to promoting human health. Further exploration and utilization of rice bran for the creation of high-value functional products is of considerable importance.

DF is the seventh essential nutrient. It serves as a promising ingredient in functional foods (Swallah et al., 2021). The primary components of DF include cellulose, lignin, hemicellulose, pectin, and oligosaccharides, all of which feature a variety of chemical structures that resist digestion by human enzymes (Begum & Deka, 2019; Xu et al., 2022). It is not easily digested or absorbed in the human small intestine. DF can improve intestinal health, regulate sugar and lipid metabolism in the body, and increase satiety. Nevertheless, it can undergo partial and complete fermentation in the large intestine. DFs can be categorized as either SDF or IDF based on solubility, which is crucial for human health and sustaining functional balance in the body (Yegin et al., 2020).

* Corresponding author: College of Food, Heilongjiang Bayi Agricultural University, Daqing 163319, China.
** Corresponding author: College of Food and Biological Engineering, Qiqihar University, Qiqihar 161006, China
E-mail addresses: liuxiaolan001@126.com (X. Liu), zhengxiqun@126.com (X. Zheng).
[1] The first and second authors contributed equally to this work.

https://doi.org/10.1016/j.fochx.2024.101975
Received 14 September 2024; Received in revised form 30 October 2024; Accepted 5 November 2024
Available online 9 November 2024

Currently, extracted rice bran dietary fiber is predominantly dominated by IDF, with a small proportion comprising SDF. In general, two different dietary fibers exert their activities in different ways. SDF has been demonstrated to regulate blood sugar levels and reduce cholesterol due to its high viscosity and adsorption capacity. In contrast, IDF has been demonstrated to improve constipation and prevent obesity due to its good water-holding and oil-holding properties (Zhang, Wu, et al., 2023). Investigating the influences of various modification techniques on the properties of DF sourced from rice bran is essential for further improving its physicochemical and functional qualities.

The appropriate modification of DF can lead to enhancement in the content, physicochemical characteristics, and functional characteristics of either SDF or IDF. Applying γ-irradiation as a novel food processing and sterilization technology has attracted increased attention, primarily due to its straightforward operational nature, brief treatment duration, extensive treatment capacity, convenient control, and the absence of chemical substance requirements and environmental pollution (Cheng et al., 2022; Sunder et al., 2022). Applying γ-irradiation can prolong the shelf life of food items by modifying the microstructure of substance molecules, thereby altering the physicochemical properties of substances. Moreover, γ-irradiation is safe and not radioactive (Chen, Zhou, et al., 2023). The breakdown of polysaccharides using physical techniques like γ-irradiation provides specific benefits, allowing for consistent and measurable alterations without requiring specialized tools or chemical substances (Hojjati et al., 2023). Additionally, enzymatic methods exhibit high specificity, mild processing conditions, high efficiency, stable processing, and environmental compatibility. It has been demonstrated that enzymatic methods can enhance the bioactivity of DF by altering the bran structure or rearranging the internal composition, thereby increasing the exposure sites of functional groups and consequently improving DF bioactivity (Song et al., 2018). Zhu et al. (2022) found that the application of the γ-irradiation modification method resulted in addition to significant improvements in the SDF content of soybean hulls, as well as notable enhancements in the *in vitro* total energy digestion and glycemic reduction capabilities. The former exhibited a 342.88 % improvement, while the latter demonstrated a 117.02 % enhancement (Zhu et al., 2022). Ma et al. (2022) observed that cellulase / xylanase modification increased the soluble monosaccharide content, as well as enhanced thermal stability and functional properties (WHC, OHC, SC, adsorptivity) of potato DF (Ma et al., 2022).

Although γ-irradiation and enzymatic methods have been demonstrated to exert a significant impact on the enhancement of polymeric materials' biological properties, the impact of their combined action on the structural and functional attributes of DF has yet to be extensively documented. Accordingly, the purpose of this research was to evaluate the physicochemical properties, functional qualities, prebiotic potential, and antidigestive capacity of rice bran DF through the combination of γ-irradiation and an enzymatic method, and to analyze the correlation between the indexes through the utilization of clustered thermograms and correlation thermograms, with the intention of to identify an optimal modification method for rice bran extracted DF. Offer a favorable endorsement for the extensive use of by-products from rice bran processing.

2. Materials and methods

2.1. Materials

The defatted rice bran was supplied by Wanyuan Oils and Fats Co. Technology Ltd. (Suihua, China). *Lactobacillus plantarum* (BNCC192575) and *Lactobacillus acidophilus* (BNCC336636) were obtained from Bei Na Biotechnology Co. Ltd. (Beijing, China). The cellulase (2×10^6 U/g), xylanase (1×10^5 U/g), alkaline protease (2×10^5 U/g), α-amylase (2×10^5 U/g), and glucoamylase (1.5×10^5 U/g) were procured from DOING HIGHER Biotechnology Co. Ltd. (Nanjing, China). The inulin was procured from Fengning Ping'an Hi-Tech Industrial Co. Sodium cholate was procured from Beijing Kubo Biotechnology Co (Beijing, China). The modified MRS medium (MMB) was procured from Qingdao Risui Biotechnology Co (Qingdao, China).

2.1.1. Preparation of DF from rice bran

The method was based on Liu with minor adjustments (Liu et al., 2020). The raw material was processed according to the literature method, then water was added at a ratio of 1:12 (g/mL), and the pH was adjusted to 6.5. 1 % α-amylase was added and the mixture was heated at 60 °C for 1 h to facilitate hydrolysis, after which it was boiled to deactivate the enzyme. The temperature was lowered to 55 °C to adjust the pH of the mixture to 9.0, 2 % alkaline protease was added and the hydrolysis time was 2 h. Subsequently, the enzyme was inactivated by reheating the mixture. After lowering the temperature to 50 °C, the pH was adjusted to 4.2. The glucoamylase at a concentration of 1 % was added and allowed to hydrolyze for 2 h, after which the enzyme was deactivated once more. Then centrifuge (1300 ×*g*, 10 min) and the precipitate was lyophilized to obtain IDF, which was recorded as CR-IDF. The supernatant was reduced in volume to 1/3 of its initial amount using both vacuum and decreased pressure and then SDF was precipitated using adding 4 times the volume of 95 % ethanol for 10 h at 4 °C. The precipitate was centrifuged, retained, and lyophilized to obtain SDF, which was CR-SDF.

2.1.2. γ-Irradiation-enzymatic modification of DF from rice bran

The modification process was conducted by the approaches proposed by Li and Ren. (Li et al., 2022; Ren et al., 2021), with slight adaptations. The pretreatment of skimmed rice bran was conducted by the aforementioned methodology, and the resulting powder was irradiated with Co γ-rays at a dose of 10 kGy (Furui High Energy Technology Co., Ltd., Guangzhou, China). The dose was determined using an alanine dosimeter (Bruker Instruments, Rheinstetten, Germany), with measurement conducted using a Bruker EMS 104 EPR analyzer. The irradiated sample is kept in a sealed bag at ordinary temperature. The sample was mixed with water at 1:12 (g/mL). The pH 5.0 level was regulated to 5.0, 2 % cellulase and 1 % xylanase were added, and hydrolysis was performed at 50 °C for 3 h. The enzymes were deactivated by boiling the mixture. Subsequently, the components, including starch and protein, were removed sequentially as previously described, resulting in the production of the IDF and SDF, which were labeled IR-IDF and IR-SDF, respectively.

2.1.3. Particle size and color

The distribution of particle sizes in the samples was evaluated using a laser particle size analyzer (Mastersizer 3000, Malvern, UK). Furthermore, use a colorimeter (CR-10 Plus, Tokyo, Japan) to analyze the color characteristics of the sample. Observe the L*, a*, and b* values of the sample (corresponding to brightness, red, and yellow, respectively) to gain a deeper understanding of its color properties.

2.1.4. Monosaccharide composition

An Agilent 1220 high-performance liquid chromatograph (manufactured in California, USA) was utilized, and the determination was conducted by the methodology proposed by Ren (Ren et al., 2021). 10 mg of the sample was placed into a 10 mL ampoule for acid hydrolysis (trifluoroacetic acid). Then, an additional hydrolysis step was conducted out by adding 4 mL of NaOH (2 mol/L) to the sample hydrolysate in an EP tube, along with 500 μL of 0.4 mol/L PMP-methanol mixture at 70 °C for 1 h. After that, add 500 μL of 0.3 mol/L HCl to neutralize the mixture. The excess derivative reagent was removed by chloroform extraction and repeated 3 times. The sample was then subjected to HPLC analysis after filtration employing a filter membrane with 0.22 μm. A C18 analytical column, and mobile phase A: phosphate buffer, B: acetonitrile. The injection is 20 μL with a current velocity of 1.0 mL/min. The column temperature is 30 °C, and the measured wavelength is 250 nm.

2.2. Structural characterisation

2.2.1. Scanning electron microscope (SEM)

The sample needs to undergo spray gold treatment, and then the microstructure of the sample was observed using scanning electron microscopy (S4800, Hitachi Ltd., Tokyo, Japan) under an acceleration voltage of 10 kV.

2.2.2. Fourier transformed-infrared spectroscopy (FT-IR)

The sample (3 mg) was blended with dehydrated potassium bromide (300 mg) and made into thin slices. The spectral range of 400 to 4000 cm^{-1} was analyzed with an FTIR spectrometer (Bruker, Ettlingen, Germany).

2.2.3. X-ray diffraction (XRD)

The crystal structure of the samples was determined by X-ray diffraction (D8 Advance A25, Bruker, Karlsruhe, Germany). The 2θ range was 5–60°, with a detection rate of 0.02.

2.2.4. Thermal (TG-DTG)

The 15 mg sample was subjected to a thermal analysis, whereby it was warmed from 25 °C to 600 °C, 10 °C/min (nitrogen), applying a thermal analyzer (NETZSCH, Sebul, Germany).

2.3. Physico chemical property

2.3.1. Water holding capacity (WHC)

A 0.5 g sample was weighed and wholly blended with 50 mL of water. The mixture was agitated at ordinary temperature for 2 h and left to sit for an additional 12 h. Following this, centrifugation (1300 ×*g*, 10 min) and record the wet sediment quality.

$$\mathrm{WHC\ (g/g)} = \frac{W_e - W_d}{W_d} \tag{1}$$

where W_e denotes the wet weight of centrifugal precipitation, whereas W_d indicates the sample weight.

2.3.2. Oil holding capacity (OHC)

A 0.5 g sample was weighed and wholly blended with 50 mL of soybean oil. The resulting solution was then left at ordinary temperature for 4 h. Following this, centrifugation (1300 ×*g*, 10 min) and record the wet sediment quality.

$$\mathrm{OHC\ (g/g)} = \frac{W_f - W_d}{W_d} \tag{2}$$

where W_f denotes the wet weight of centrifugal precipitation, whereas W_d indicates the sample weight.

2.3.3. Swelling capacity (SC)

Weigh 0.5 g of sample and wholly blended with 50 mL of water. The solution was then left to sit at ordinary temperature for 24 h. The initial volume of the sample solution was noted, as was the volume after water absorption and swelling had occurred.

$$\mathrm{SC\ (mL/g)} = \frac{V_0 - V_1}{W_S} \tag{3}$$

where V_0 denotes the volume of the sample after water absorption and expansion, V_1 denotes the original volume of the sample, and W_s denotes the mass of the dried sample.

2.3.4. Glucose adsorption capacity (GAC)

The approach proposed by Jiang was referenced and adjusted minimally (Jiang et al., 2024). Weigh 0.5 g of sample and mixed with 50 mL of glucose solutions with concentrations of 50, 100, and 150 mmol/L. The mixture was shaken at 37 °C (150 rpm, 6 h), then centrifuged (1300 ×*g*, 10 min). Use a kit method to determine the glucose content in the supernatant.

$$GAC\ \mathrm{(mmol/L)} = \frac{N_2 - N_3}{W_S} \tag{4}$$

where N_2 indicates the initial glucose content, N_3 indicates the final glucose content following the completion of the reaction, and W_s signifies the mass of the dried sample.

2.3.5. Cholesterol adsorption capacity (CAC)

The approach proposed by Zheng was referenced, with little changes (Zheng et al., 2022). Weigh 0.5 g of sample and mixed with 50 mL of egg yolk diluent, diluted by volume to a ratio of 1:9 with water. To simulate the acidic gastric and neutral intestinal environments, the pH of the mixture was adjusted to 2.0 / 7.0, separately. The samples were shaken at 37 °C (150 rpm, 4 h), then centrifuged (1300 ×*g*, 10 min). The cholesterol content in the supernatant was determined using the o-phthalaldehyde approach.

$$CAC\ \mathrm{(mmol/L)} = \frac{N_4 - N_5}{W_S} \tag{5}$$

where N_4 represents the initial cholesterol content, N_5 represents the cholesterol content after adsorption, and Ws represents the mass of the dried sample.

2.3.6. Sodium cholate adsorption capacity (SCAC)

Refer to the approach proposed by Yang and make slight adjustments (Yang et al., 2021). The sample was weighed at 0.5 g, and 50 mL of a sodium cholate solution at a concentration of 0.75 mg/mL were mixed. The pH of the resulting mixture was set to 2.0 / 7.0. To imitate the *in vitro* gastrointestinal environment, the sample was shaken at 37 °C (150 rpm, 3 h), then centrifuged (1300 ×*g*, 10 min). The resulting supernatant was then used in the furfural colorimetric assay to determine the sodium cholate content of the sample.

$$\mathrm{SCAC\ (mg/g)} = \frac{M_0 - M_1}{W_S} \tag{6}$$

where M_0 represents the initial sodium cholate content, M_1 denotes the sodium cholate content after adsorption, and W_s denotes the mass of the dried sample.

2.4. Biological activity

2.4.1. In vitro antidigestive characterisation

The *in vitro* antidigestive properties of the samples were evaluated by preparing artificial gastric fluid and artificial intestinal fluid using the methodology outlined by Zhang (Zhang, Xu, et al., 2023). A quantity of 0.2 g of inulin, CR-SDF, IR-SDF, CR-IDF, and IR-IDF to an Erlenmeyer flask containing 20 mL of artificial gastric / intestinal juice and adjusted the pH to 2.0 / 7.0. The samples were incubated in a 37 °C water bath for 6 h. Measure the total sugar and reducing sugar content at 0, 1, 2, 3, 4, 5, and 6 h of digestion, respectively. The total sugar content was determined by the phenol sulfate approach, and the reducing sugar content was determined by the DNS approach.

$$\mathrm{Hydrolysis\ rates\ (\%)} = \frac{m_b - m_a}{m_c - m_a} \tag{7}$$

where m_c signifies the total sugar content (mg) present in the sample before digestion, m_a signifies the reduced sugar content (mg) present in the sample before digestion, and m_b signifies the reduced sugar content (mg) present in the sample following digestion.

2.4.2. In vitro probiotic activity

The method employed here is founded on the description by Tian with minor adjustments (Tian et al., 2023). The *in vitro* probiotic activity

of the samples was assessed. The following samples were added to the MMB medium at a 2 % mass fraction: glucose (negative control), inulin (positive control), CR-SDF, IR-SDF, CR-IDF, and IR-IDF. These samples were dissolved by thorough shaking and subjected to autoclaving at 121 °C for 15 min. *Lactobacillus acidophilus* and *Lactobacillus plantarum* were inoculated in 10 mL of sterilized MRS medium and incubated for 16 h. After that, 1 mL of the activated bacterial liquid was taken and inoculated into an MMB medium, supplemented with glucose, inulin, CR-SDF, IR-SDF, CR-IDF, and IR-IDF, respectively. Furthermore, a culture medium devoid of any carbon source was employed as a control (MMB), and cultivated at 37 °C for 56 h (anaerobic constant temperature incubator).

(1) Determination of growth curves

At 0, 6, 12, 18, 24, 30, 36, 42, 48, and 54 h fermentation nodes, the fermentation broth (2.0 mL) was taken in sterile centrifuge tubes and centrifuged (424 ×*g*, 2 min) to remove the sediment, thereby retaining the supernatant. Using a blank control as a reference. Measure wavelength: 600 nm (96 well plate) and plot growth curve.

(2) pH measurement.

Use a pH meter to measure the pH of the supernatant in (1).

(3) Determination of total acid content.

A volume of 0.2 mL from the sample (1) was transferred to a sterile conical flask. After that, 4 mL of distilled water was incorporated, and phenolphthalein (200 μL) as a color developer. Titration solution: NaOH (0.01 mol/L), and when the reaction solution gradually turns pink and does not fade within 30 s, it is the endpoint of titration. Record the volume of NaOH solution consumed.

2.4.3. Data analysis

The data in this experiment were averaged from three parallel experiments ($n \geq 3$). Analysis of variance was performed on the data using SPSS 27 statistical software. Multivariate analysis of the data was performed using cluster analysis, PCA, and correlation heat map analysis. The graphs were plotted using Origin 2024b.

3. Results and discussion

3.1. Yield analysis

Fig. 1 illustrates that the yields of SDF and IDF prepared using defatted rice bran were (9.18 ± 0.32) g/100 g and (58.11 ± 1.07) g/100 g, respectively, and the TDF yield is (67.28 ± 1.15) g/100 g. The integration of γ-irradiation along with enzymatic modification led to remarkable enhancement in the yield of SDF ($P < 0.05$), while the yield of IDF diminished ($P < 0.05$), with yields of (13.38 ± 0.40) g/100 g and (52.19 ± 0.97) g/100 g, separately. The yield of TDF was found to be (65.57 ± 1.04) g/100 g. It can be hypothesized that the modification mechanism causes some IDF to be converted into SDF. It has been demonstrated that γ-irradiation is capable of destroying hydrogen bonds and van der Waals forces between and within molecules, which affects the stability of polysaccharide chains (Li et al., 2022). Furthermore, insoluble long-chain cellulose is decomposed into smaller soluble fragments by enzymatic hydrolysis, which increases the SDF content (Sun et al., 2021).

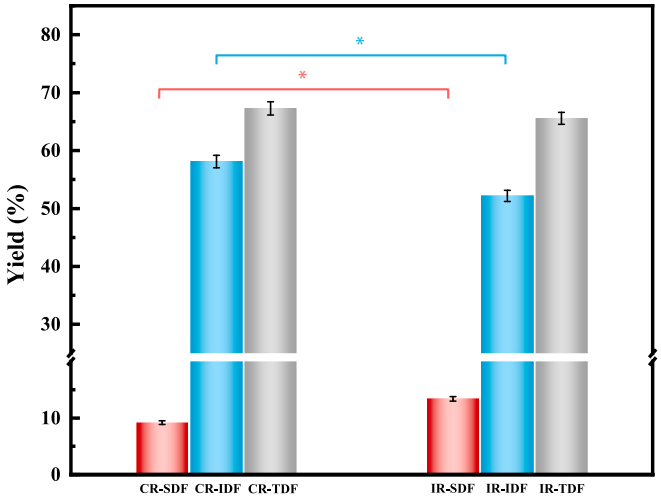

Fig. 1. Yields of dietary fiber from rice bran prior to and following modification. CR-SDF, unmodified SDF; IR-SDF, γ-irradiation-enzyme hydrolysis modification SDF; CR-IDF, unmodified IDF; IR-IDF, γ-irradiation-enzyme hydrolysis modification IDF.* indicates a noteworthy distinction ($P < 0.05$).

3.1.1. Particle size and color analysis

Table 1 illustrates that the combination of γ-irradiation and enzymatic modification can markedly reduce the particle size of SDF and IDF. This is accompanied by a corresponding decrease in the surface average particle size (D[3,2]) and volume average particle size (D[4,3]), while the specific surface area (SSA) increases. The greater the dispersibility, the more favorable the solubility in the food system. The increase in the specific surface area of dietary fibers provides more contact sites for hydrogen bond donors and acceptors, thereby enhancing the water-holding capacity of the modified DF. Hydrogen bonds can also help maintain the three-dimensional structure of dietary fiber, enabling it to effectively adsorb and transport cholesterol and excess glucose in the digestive system, which has potential benefits for the prevention of

Table 1
Changes in particle size, color, and monosaccharide composition of SDFs and IDFs prior to and following modification.

	CR-SDF	IR-SDF	CR-IDF	IR-IDF
Particle size (μm)				
D10	2.56 ± 0.03^{a}	2.46 ± 0.15^{a}	4.60 ± 0.27 ^{A}	4.39 ± 0.16^{B}
D50	23.53 ± 0.03^{a}	17.51 ± 0.03^{b}	23.88 ± 0.17 ^{A}	23.48 ± 0.42 ^{A}
D90	91.65 ± 0.34^{a}	83.60 ± 0.42^{b}	73.39 ± 0.45 ^{A}	70.13 ± 0.21^{B}
D[3,2]	7.11 ± 0.35^{a}	6.05 ± 0.21^{b}	10.79 ± 0.55 ^{A}	10.35 ± 0.36 ^{A}
D[4,3]	36.90 ± 0.74^{a}	31.74 ± 0.44^{b}	32.61 ± 0.73 ^{A}	31.45 ± 0.26^{B}
Specific surface area (m^2/g)	0.27 ± 0.01^{b}	0.32 ± 0.01 ^{A}	0.18 ± 0.01 ^{A}	0.19 ± 0.01 ^{A}
Color				
L*	87.63 ± 1.02^{a}	84.23 ± 0.63^{b}	74.79 ± 0.76^{B}	77.54 ± 0.33 ^{A}
a*	3.54 ± 0.52^{b}	4.81 ± 0.18^{a}	6.75 ± 0.06 ^{A}	5.86 ± 0.06^{B}
b*	14.31 ± 0.73^{b}	16.74 ± 0.35^{a}	21.41 ± 0.14 ^{A}	19.03 ± 0.07^{B}
Main monosaccharides (Molar ratio, %)				
Mannose	1.83	2.73	1.53	1.33
Ribose	0.36	0.72	0.52	0.54
Rhamnose	2.10	1.49	1.38	1.04
Glucuronic acid	1.31	1.84	0.70	0.85
Galacturonic acid	6.10	4.43	1.13	1.06
Glucose	76.03	63.18	45.51	47.79
Galactose	4.87	4.86	5.10	4.61
Xylose	1.24	7.92	22.43	22.29
Arabinose	5.52	11.66	20.88	19.61
Fucose	0.65	1.19	0.82	0.88

The appearance of different letters next to the same metric for SDF and IDF indicates a significant difference between the data ($P < 0.05$). The discrepancies between SDF are indicated by lower-case letters, while differences between IDF are indicated by capital letters.

chronic diseases such as obesity, diabetes, and intestinal disorders (Barber et al., 2020). This physical modification strategy effectively enhances the potential of dietary fibers for use in food processing and biomedical applications.

Before and following the modification, there were notable contrasts in the color and brightness of the SDF and IDF Table 1. The IR-SDF sample exhibited a decrease in L* value (brightness) and an increase in a* (red) and b* (yellow) compared to the CR-SDF sample. In comparison to CR-IDF, IR-IDF exhibited an increase in L* value (brightness) and a diminish in a* (red) and b* (yellow). The alteration in the hue of the material may be attributed to fluctuations in the concentration of soluble pigments and proteins present in the rice bran during the modification procedure.

3.1.2. Monosaccharide composition analysis

Table 1 illustrates the monosaccharide composition of rice bran SDF and IDF both prior to and following modification. Rice bran SDF is primarily constituted of glucose, arabinose, xylose, galactose, and galacturonic acid. After γ-irradiation combined with enzymatic modification, the content of glucose and galacturonic acid decreased. It was also noted that the alteration in glucose content was frequently correlated with changes in the cellulose structure of the resulting DF (Ma et al., 2015). This suggests that the cellulose structure, as well as galacturonic acid, which constitutes the fundamental backbone of the pectin structure, may undergo partial degradation during the modification process. The elevated content of arabinose and xylose indicates that part of the cellulose and pectin structure was destroyed to form hemicellulose during the modification process. Furthermore, the action of cellulase and xylanase enzymes resulted in alterations to the monosaccharide composition of SDF. The main monosaccharide components in the rice bran IDF are glucose, arabinose, and galactose in order. After modification, the proportion of xylose and arabinose slightly decreased, while the proportion of glucose slightly increased. Therefore, further inference is made that the monosaccharide composition is closely related to the structure and functional activity of DF (Tang et al., 2024).

3.2. Structural-characterisation analysis

3.2.1. SEM analysis

Fig. 2 displays the SEM graphics of rice bran SDF and IDF prior to and following modification at different magnifications. Compared to the pre-modified DF, the internal structure of the modified DF is loose, with more fragments formed on the surface, resulting in greater spatial porosity and an increase in specific surface area. Previous research has confirmed that irradiation has a damaging effect on dietary fiber particles, effectively degrading cellulose and hemicellulose in soybean fiber,

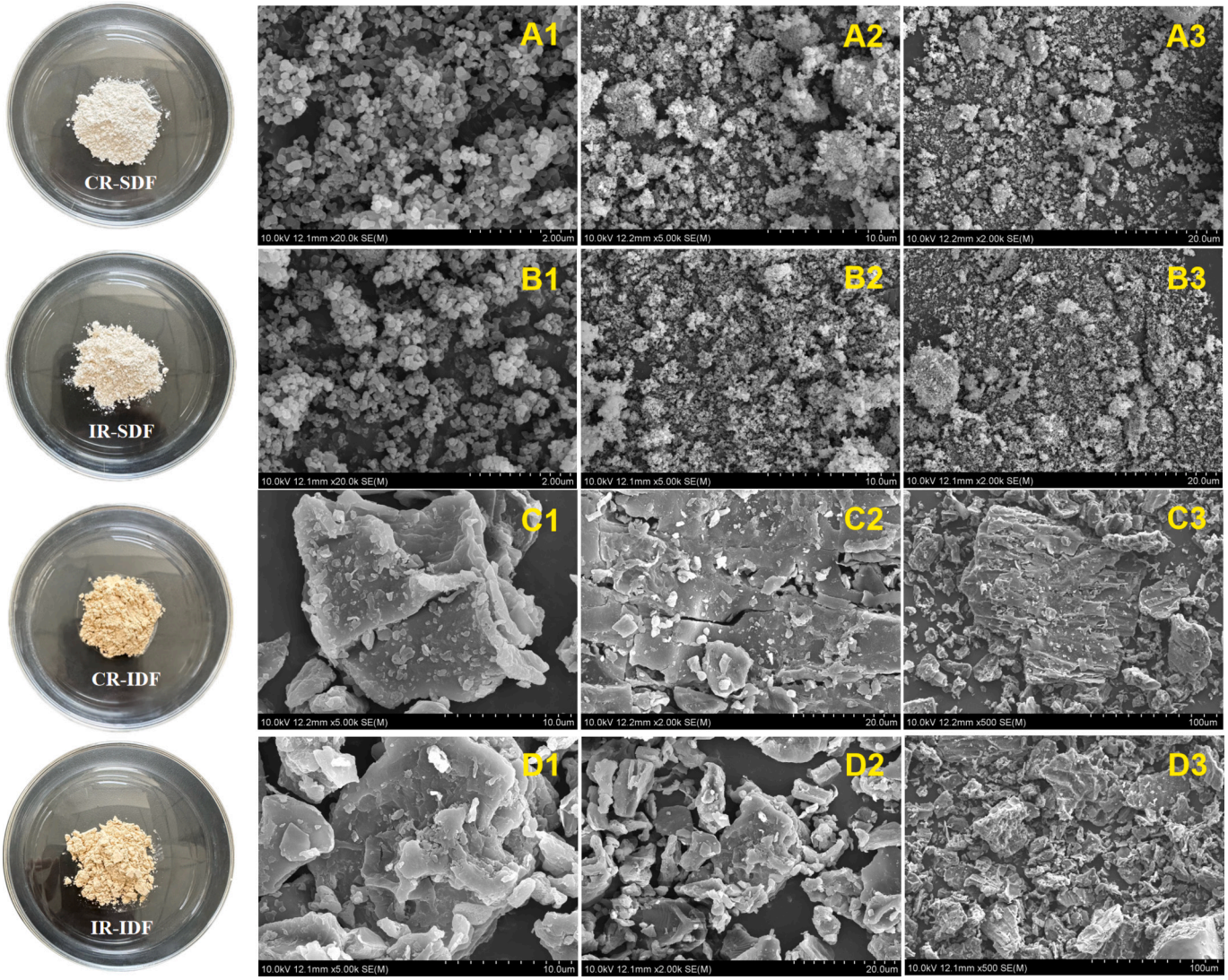

Fig. 2. CR-SDF: A1-A3(20,000×, 5000×, 2000×); IR-SDF:B1-B3(20,000×, 5000×, 2000×); CR-IDF:C1-C3 (5000×, 2000×, 500×); IR-IDF:D1-D3 (5000×, 2000×, 500×).

and leading to more pronounced cracks on the fiber surface (Li et al., 2022; Zhu et al., 2022). In addition, more cellulase and xylanase enter the interior of the fiber, leading to an increased proportion of cellulose and lignin degradation, which further contributes to the formation of the honeycomb structure. Therefore, the modification method that combines physical modification with enzymatic hydrolysis can significantly improve the hydrolysis efficiency compared with a single modification process.

3.2.2. FT-IR analysis

FT-IR spectroscopy was utilized to analyze the varies in the reactive groups of rice bran DF molecules before and after γ-irradiation combined with enzymatic modification, and compared with the relevant literature (Hua et al., 2019; Jia et al., 2019). Fig. 3A shows the characteristic FTIR peaks of SDF and IDF prior to and following modification, and the broad absorption band centered at 3269 cm^{-1} perhaps because of the intramolecular hydrogen bond cleavage of the -OH group in the crystalline region of cellulose (Wen et al., 2017). Furthermore, the absorption peak of IDF at 2922 cm^{-1} is attributed to the C—H stretching

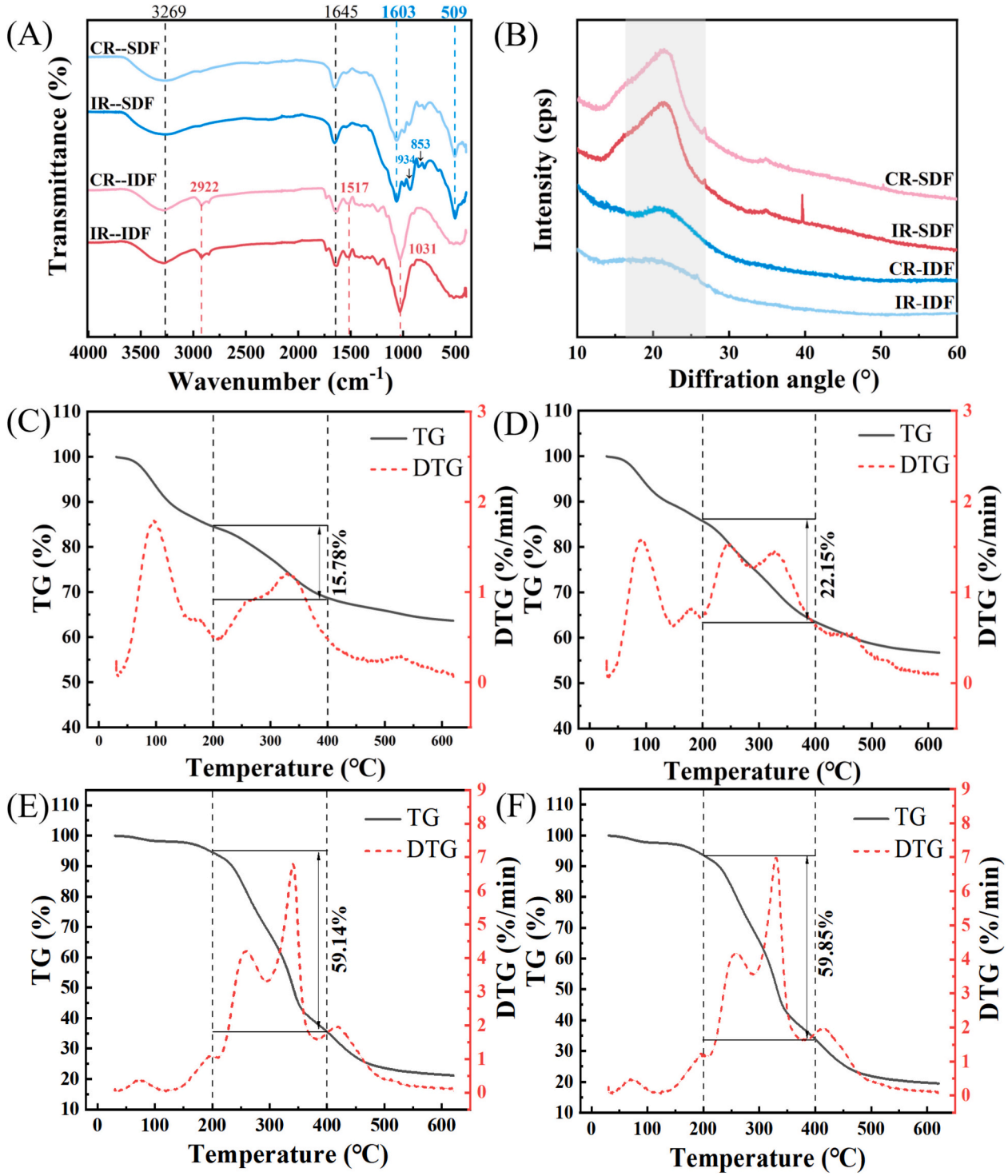

Fig. 3. (A) FTIR, (B) XRD, (C) CR-SDF thermogravimetry, (D) IR-SDF thermogravimetry, (E) CR-IDF thermogravimetry, (F) IR-IDF thermogravimetry.

vibration of methylene (Jia et al., 2019). The band at 1645 cm^{-1} indicates the characteristic absorption of C═O exists in uronic acid in both SDF and IDF (Chu et al., 2019). The absorption peak at 1517 cm^{-1} confirms the presence of carboxyl groups in rice bran IDF (Zhang et al., 2020). The increase in functional groups (hydroxyl and carboxyl groups) can impart better functional properties to dietary fibers. The peaks at 1063 cm^{-1} and 1031 cm^{-1} indicate that both SDF and IDF contain sugar ring structures (Jiang et al., 2024).

3.2.3. XRD analysis

The crystal structure of DF has been analyzed by X-ray diffraction. Research indicates that the dietary fiber found in rice bran is a natural fiber substance, which means its cellulose crystal structure is classified as type I (Ren et al., 2021). Fig. 3B also shows that rice bran SDF before and after modification has distinct characteristic crystalline peaks around $2\theta = 21°$, which is due to cellulose type I. The diffraction peak appearing at $2\theta = 39–40°$ is also attributed to a characteristic peak of the cellulose type I structure, perhaps because of the disruption of part of the cellulose structure during the modification process (Ju et al., 2015). However, the crystal configuration of IR-SDF did not change after γ-irradiation combined with enzymatic modification, consistent with the research findings of Ren et al. (Ren et al., 2021).

The diffraction peaks of the IDF samples were predominantly located around 10 and 22°, which suggests the presence of a cellulose II configuration and a cellulose I double helix configuration, separately (Cai et al., 2019). The findings displayed no notable variation in the crystal structure of IDF prior to and following modification. The intensity of the diffraction peak at about 22° is reduced for IR-IDF compared to CR-IDF. This phenomenon may be attributed to the disruption of the irregularities observed in the hemicellulose attached to the cellulose surface following modification by the γ-irradiation binding enzyme. The improved adsorption performance of SDF and IDF after modification perhaps because of their comparatively loose structure and the interaction force is weak (Jiang et al., 2024).

3.2.4. TG-DTG analysis

TG-DTG was employed to assess the alterations in thermal stability and structural characteristics of rice bran DF before and after modification. The DTG curves in Fig. 3C-3F all have five peaks, showing the presence of distinct chemical compositions that undergo degradation at varying temperatures. The DTG plot of CR-SDF, the peak around 100 °C may be caused by water evaporation, the second peak is at 150–200 °C, possibly due to the degradation of hemicellulose (Liu et al., 2020). The third peak appears in the temperature scope for 200–300 °C, which may be related to the decomposition of hemicellulose (Khawas & Deka, 2016). The peak intensity corresponding to IR-SDF is greater than that of CR-SDF, indicating that IR-SDF has a greater hemicellulose content. The fourth peak is between 300 and 400 °C and is linked to the breakdown of cellulose (Morán et al., 2008). Therefore, at 200–400 °C, both rice bran SDF and IDF mainly suffer from the breakdown of cellulose and hemicellulose, leading to a rapid loss of quality, with IR-IDF and CR-IDF showing the greatest loss of 59.85 % and 59.14 %, respectively. The

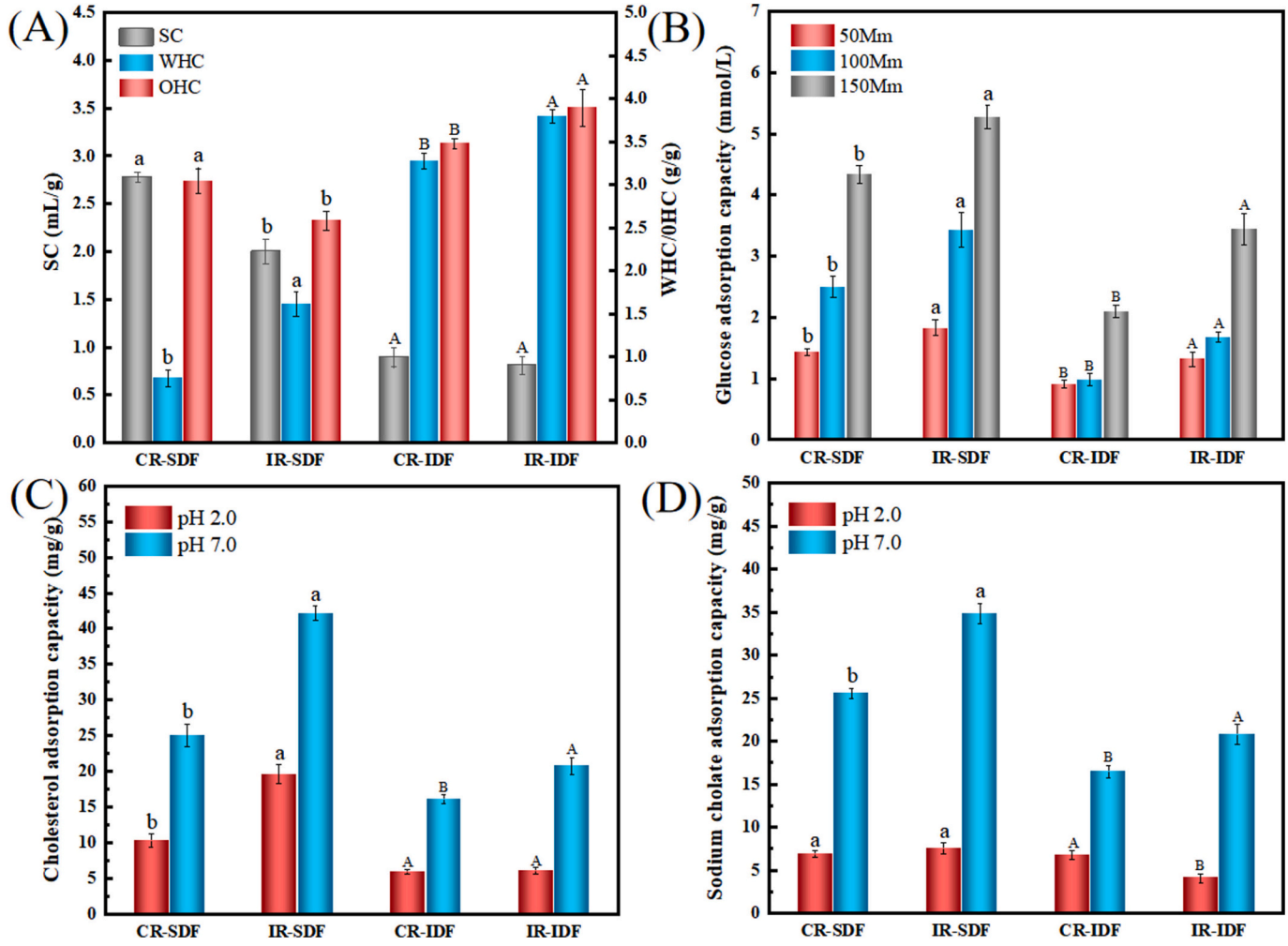

Fig. 4. (A) WHC, OHC, and SC, (B) GAC, (C) CAC, (D) SCAC. The presence of different letters following to the same indicators in the SDF and the IDF indicates a notable disparity in the data ($P < 0.05$), where the difference between the SDF is indicated by a lowercase letter and the difference between the IDF by a capital letter.

loss rates of IR-SDF and CR-SDF were 22.15 % and 15.78 %, respectively, indicating that SDF has higher stability compared to IDF. The fifth peak was located between 400 and 550 °C, presumably caused mainly by the degradation of lignin.

3.3. Physico-chemical property analysis

3.3.1. WHC, OHC, SC analysis

The results of Fig. 4A indicated that combining γ-irradiation and enzymatic modification substantially enhanced the WHC of rice bran SDF, but decreased the OHC and SC. In contrast, IR-IDF showed a noticeable increase in WHC and OHC ($P < 0.05$) and a decrease in SC. The variation of these indicators is highly dependent on the microstructure of the fibers (Zhu et al., 2022). This may be because the modification treatment increases the porosity of DF and improves its surface tension as well as the contact area with water molecules, which can penetrate more easily into more fiber structures and the WHC is significantly improved. In addition, the disruption of glycosidic bonds and degradation of polysaccharides by γ-irradiation create additional space for storing water molecules (Li et al., 2022). Due to the modification process leading to a decrease in IDF particle size, an increase in porosity and specific surface area, which is conducive to better physical oil encapsulation, thus improving its oil-holding capacity. The OHC of rice bran DF is significantly higher than that of irradiated navel orange peel (Li et al., 2022). Changes in the OHC of dietary fibers are ascribed to the existence of hydrophobic areas bound to oil, and γ-irradiation combined with enzymatic modification induces the dissociation and degradation of part of the fiber structure, which further alters the spatial structure in the oil / water system (Noguerol et al., 2022). On the contrary, even if modified fibers have more porous surfaces, the ability of the fibers to absorb water diminishes with the degradation of cellulose and hemicellulose, leading to a diminish in the water absorption and swelling ability of modified SDF and IDF (Zhu et al., 2022).

3.3.2. GAC analysis

The glucose adsorption capacity index reflects the capacity of dietary fiber to regulate blood sugar levels after a meal. It is an important functional characteristic of DF. From Fig. 4B, it can be seen that γ-irradiation combined with enzymatic modification treatment significantly increased the glucose adsorption of rice bran SDF and IDF ($P < 0.05$), and its ability to adsorb glucose was related to the glucose concentration. At 150 mmol/L, the glucose adsorption of CR-SDF and IR-SDF was (4.33 ± 0.15) and (5.27 ± 0.19) mmol/L, respectively, whereas that of CR-IDF and IR-IDF was (2.10 ± 0.10) and (3.44 ± 0.26) mmol/L, respectively. The modified SDF and IDF exhibited increases in glucose adsorption of 21.71 % and 63.81 %, separately. The improved glucose adsorption capacity can be ascribed to the augmented porosity and specific surface area of the fiber surface, this increases the number of glucose molecules that can be absorbed, thus increasing the adsorption properties of glucose.

3.3.3. CAC analysis

Cholesterol adsorption capacity is a momentous index for measuring the reduction of serum cholesterol and lipid parameters by DF. Fig. 4C shows the CAC of SDF and IDF prior to and following modification at pH 2.0 / 7.0 (simulated gastrointestinal environment), separately. It was found that in the intestine, dietary fiber has a good CAC. The CAC of the SDF is stronger than that of the IDF. At pH 7.0, the CAC of IR-SDF surpassed that of CR-SDF by a factor of 1.68, the CAC of IR-IDF is 1.29 times that of CR-IDF. The outcomes showed that γ-irradiation combined with enzymatic modification notably improved the CAC of rice bran DF, especially SDF. This phenomenon may be attributed to the modified fiber surface exhibiting a looser structure, providing a further number of associative sites for cholesterol.

3.3.4. SCAC analysis

The sorption capacity of bile salts by DF has the potential to benefit human health *via* multiple mechanisms, particularly in the prevention and management of cardiovascular conditions, the improvement of lipid metabolism, and the maintenance of intestinal health. Fig. 4D shows the SCAC of SDF and IDF prior to and following modification at pH 2.0 / 7.0 (simulated gastrointestinal environment), respectively. Both SDF and IDF were found to have a higher SCAC at pH 7.0 than at pH 2.0, probably because in the acidic environment of the stomach, bile salts exist mainly in ionic form, a form that is less able to bind with dietary fiber, whereas in the intestine, bile salts exist mainly in non-ionic form, which is more capable of interacting with the hydrophilic and hydrophobic regions of dietary fiber (Singh et al., 2019). At pH 7.0, the CAC for IR-SDF exceeded that of CR-SDF by a factor of 1.36, the CAC of IR-IDF is 1.26 times that of CR-IDF. The outcomes showed that γ-irradiation combined with enzymatic modification notably improved the SCAC of rice bran DF.

3.4. Biological-activity analysis

3.4.1. In vitro antidigestive properties

The determination of changes in polysaccharides during gastrointestinal digestion is crucial for assessing the potential biological activity of compounds and establishing biological accessibility (Yang et al., 2023). The results of *in vitro* digestion experiments Fig. 5A-5B demonstrated that the hydrolysis rate of inulin was higher than that of the four rice bran DFs in both the simulated gastric and intestinal environments *in vitro*. This suggests that dietary fibers have more favorable antidigestive properties than inulin. The antidigestive performances of IDF were significantly higher than those of SDF. The modification process affected the hydrolysis rate of rice bran DF, perhaps because the destruction of the dietary fiber structure and the creation of a loose and porous fiber surface, increasing the specific surface area of cellulose and the number of hydrolysis sites for enzymes. This led to the degradation of some cellulose and lignin, thus altering the hydrolysis rate of rice bran DF.

3.4.2. In vitro probiotic activity

Lactobacillus acidophilus and *Lactobacillus plantarum*, two common probiotics, can assist in preserving the equilibrium of microorganisms in the intestinal tract and can decrease the population of harmful bacteria in the intestinal tract and protect the health of the intestinal tract by competing with and inhibiting the growth of harmful bacteria. Consumption of fiber-rich foods or supplements can provide the nutrients needed by probiotics to promote gut health. In the present study, the ability of two probiotics to utilize rice bran dietary fiber in MMB medium without a carbon source was assessed and contrasted with glucose and inulin as carbon sources Fig. 5C-5H. *Lactobacillus acidophilus* and *Lactobacillus plantarum* thrive quickly in a culture medium using glucose as a carbon source at 0–24 h and 0–18 h, separately. It was found that the growth-promoting effect of IR-SDF as a carbon source on *Lactobacillus acidophilus* and *Lactobacillus plantarum* was similar to that of inulin, but more persistent than inulin, indicating that the modified SDF was more readily utilized by probiotic bacteria and enhanced its potential as a prebiotic. This could be due to the effective degradation of polysaccharides in rice bran by γ-irradiation combined with enzymatic modification. SDF has better solubility, which significantly improves the bioavailability of its IR-SDF.

As can be seen from Fig. 5E-5F, the pH of the blank medium decreased only a minimal decline, whereas the pH of the medium including glucose, inulin, and different DFs reduced slowly, with a rapid decrease in the initial phase due to the rapid growth in the amount of viable bacteria and a rise in total acid production. However, the rate of increase in the quantity of viable bacteria slowed down and the pH value showed a slow decrease as the growth of probiotics was inhibited by an overly acidic environment. It indicates that rice bran SDF modified by γ-irradiation combined with the enzymatic method is better utilized by

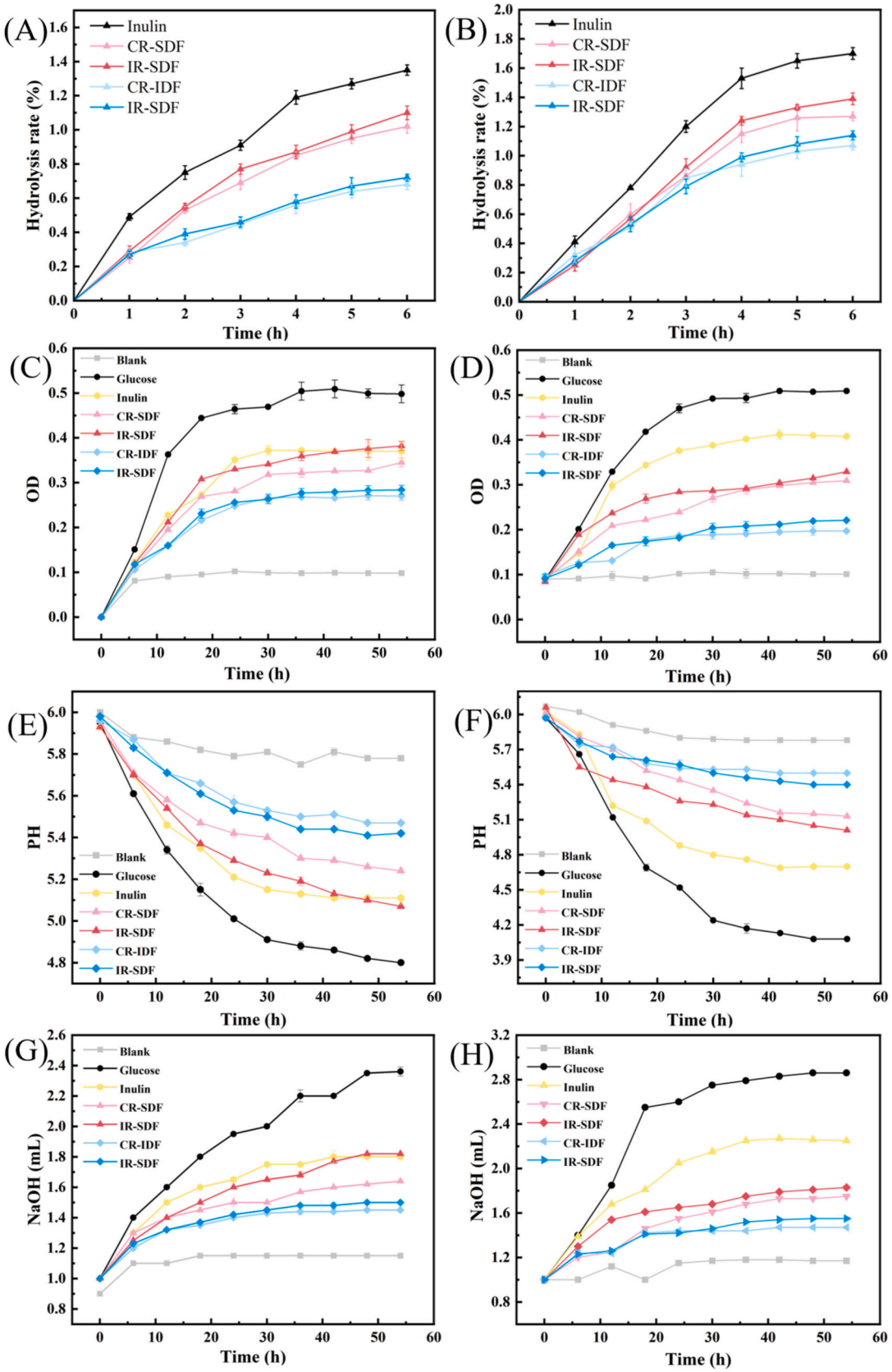

Fig. 5. (A) *In vitro* antidigestive properties in a simulated gastric environment, (B) *in vitro* antidigestive properties in a simulated intestinal environment, (C) growth curve of *Lactobacillus acidophilus*, (D) growth curve of *Lactobacillus plantarum*, (E) pH changes in *Lactobacillus acidophilus* culture, (F) pH changes in *Lactobacillus plantarum* culture, (G) NaOH consumption by *Lactobacillus acidophilus*, (H) NaOH consumption by *Lactobacillus plantarum*.

probiotics, and produces more free acid. Lowering the pH value of the culture medium can repress the proliferation of harmful bacteria in the gut.

In general, total acidity includes free and non-free acids. Consequently, the determination of the acid-producing capacity of probiotics is influenced by distinct carbon sources, which is a crucial indicator for the determination of the acid-producing capacity of probiotics (Tian et al., 2023). As can be seen from Fig. 5G-5H, the total acid content did not vary prominently in the blank medium, but remarkable changes were observed in the culture medium using rice bran DF or inulin as carbon sources, but significantly lower than those containing glucose as carbon source. The more the total acid content, the more pronounced the suppressed effect on the reproduction of harmful bacteria. The findings represented that the total acid content in IR-SDF was the highest among the four rice bran DFs.

3.5. Multivariate analysis

In this paper, clustering heatmaps are used to show the differences between different groups of data. Fig. 6A shows the clustering results of the data of four different DFs, CR-SDF, IR-SDF, CR-IDF and IR-IDF, which were divided into two main categories in total, the first major category included thermal stability, particle size (D90), SC, SSA, some indicators of probiotic activity (promoting growth activity and total acid yield), L*, intragastric antidigestive properties (GJ), and adsorption properties (SCAC (pH 7), GAC, and CAC), in which the IR-SDF group had a deeper color than the other groups, indicating higher values of the relevant indicators. After modification, IR-SDF showed a significant improvement compared to CR-SDF. In addition, D[4,3], intragastric antidigestive properties (IJ), and SCAC (pH 2) were included in the first major category, and the numerical regularities of the different groups did not significantly change. In the second major category, rice bran IDF exhibits better characteristics than SDF in yield, WHC, and OHC.

As illustrated in Fig. 6B, the findings of the principal component analysis demonstrated that the principal component (PC 1) accounted for 80.5 % of the total variance, while PC 2 accounted for 12.0 %. Additionally, CR-IDF and IR-IDF were situated on the negative side of the PCA 1 axis, whereas CR-SDF and IR-SDF were positioned on the positive side of the PCA 1 axis. The physicochemical properties of SDF were found to be superior to those of rice bran IDF, with IR-SDF demonstrating a higher positive correlation for PC 1. Furthermore, the PCA biplot illustrates that the acid production by *Lactobacillus acidophilus*, SSA, growth-promoting activity of *Lactobacillus acidophilus* and *Lactobacillus plantarum* exhibited a solid and positive loading on principal component 1 (PC1). The medium pH and D[3,2] of *Lactobacillus acidophilus* exhibited an extensive negative loading on PC1. Meanwhile, the D[4,3], D90, D50, and water absorption swelling have a large positive loading on principal component 2 (PC2). While WHC, acid production of *Lactobacillus plantarum* were large negative loadings on PC2.

The study examined the connection between the composition of monosaccharides and the physicochemical characteristics of DF by employing Pearson relationship analysis. As illustrated in Fig. 6C, the outcomes revealed a positive relationship significantly between the contents of mannose, rhamnose, glucuronic acid, galacturonic acid, and glucose with the majority of DF functional properties ($P < 0.05$), including SC, GAC, CAC, SCAC, thermal stability, antidigestive properties, probiotic growth-promoting properties, and acid production. Conversely, there was a notable negative correlation between WHC, OHC, and probiotic medium pH changes and the aforementioned variables ($P < 0.05$). The findings of the extant studies corroborate the assertion that DF prepared through disparate modification techniques typically engender alterations in their physicochemical attributes, likely attributable to modifications in their monosaccharide composition.

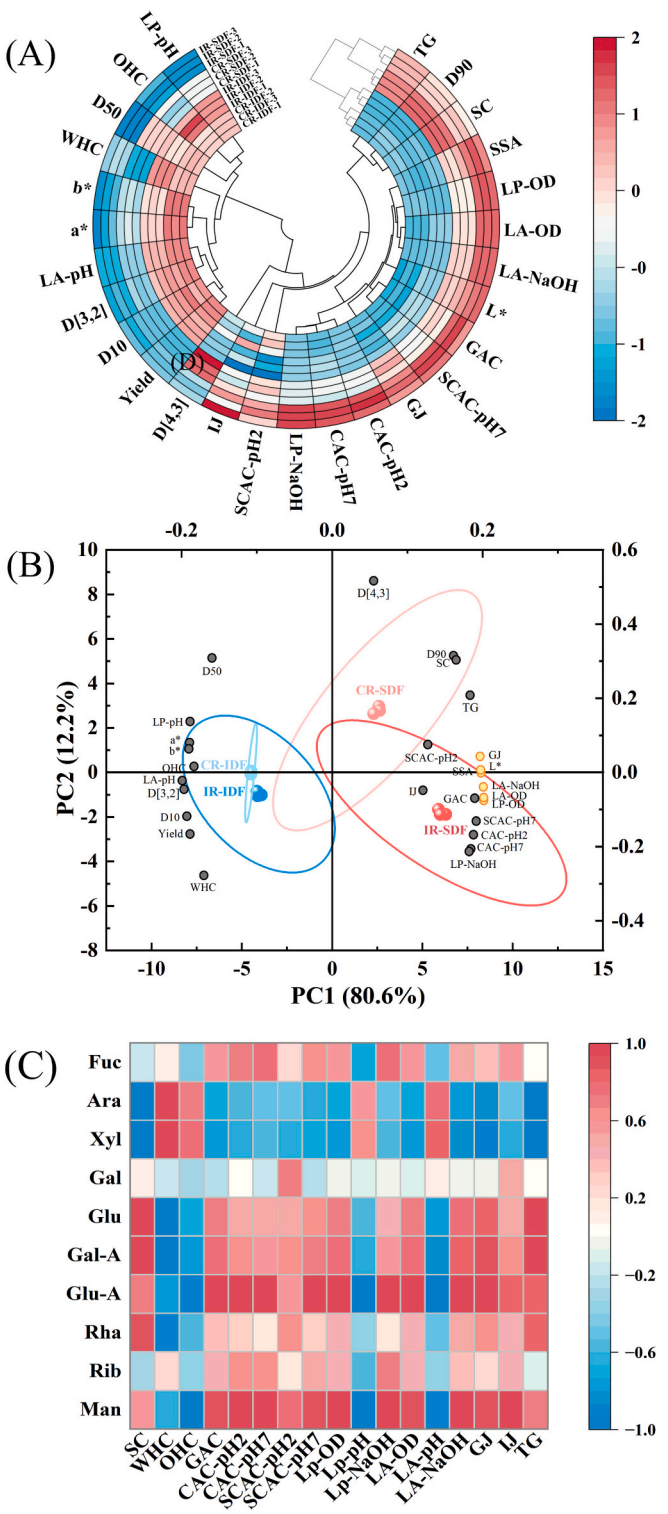

Fig. 6. (A) Clustering heatmap, (B) principal component analysis, (C) correlation matrix heatmap. Man: mannose, Rib: ribose, rha: rhamnose, glu-A: glucuronic acid, gal-A: galacturonic acid, glu: glucose, Gal: galactose, Xyl: Xylose, ara: arabinose, fuc: fucose, GJ: simulated gastric environment, IJ: simulated intestinal environment, LA-OD: *Lactobacillus acidophilus*-growth curve, LA-pH: *Lactobacillus acidophilus*-pH, LA-NaOH: *Lactobacillus acidophilus*-acid production, LP-OD: *Lactobacillus plantarum*-growth curve, LP-pH: *Lactobacillus plantarum*-pH, LP- NaOH: *Lactobacillus plantarum*-acid production, TG: weight loss.

4. Conclusion

It was demonstrated that rice bran DF modified by γ-irradiation in conjunction with an enzymatic method exhibited notable enhancements in yield, hydration, adsorption, antidigestive, and probiotic activity. Additionally, the modification process led to the emergence of distinctive mechanisms that contributed to the enhanced performance of rice bran SDF and IDF. The thermal stability, D90, swelling capacity, SSA, probiotic growth-promoting activity, total acid yield, and intestinal antidigestive properties of rice bran SDF were significantly enhanced following modification. Furthermore, rice bran IDF exhibited notable superiority over SDF in yield, WHC, and OHC. Principal component analysis demonstrated that the modified rice bran DF exhibited superior physicochemical properties, particularly in the case of rice bran SDF. Correlation analysis revealed that the contents of mannose, rhamnose, glucuronic acid, galacturonic acid, and glucose were significantly and positively correlated with the majority of the functional properties of DF ($P < 0.05$). Therefore, the availability of rice bran can be improved by γ-irradiation combined with enzymatic modification, which offers a scientific foundation for better and effective utilization of rice bran. In the future, it may be necessary to continue expanding the scale of sample preparation and to determine the mechanism by which DF exerts its specific functional characteristics through *in vivo* experiments.

CRediT authorship contribution statement

Xuyao Wei: Validation. **Caixia Jiang:** Writing – review & editing. **Xiaolan Liu:** Funding acquisition. **Handong Liu:** Investigation. **Juntong Wang:** Supervision. **Xiqun Zheng:** Writing – review & editing. **Zhi Zhang:** Conceptualization. **Hao Hu:** Conceptualization.

Declaration of competing interest

The authors declare that they have no known competing financial interests or personal relationships that could have appeared to influence the work reported in this paper.

Acknowledgments

This study was supported by the National Key Research and Development Project (2021YFD2100902); the Major Science and Technology Project of Heilongjiang Province (2021ZX12B09-4); and Heilongjiang Bayi Agricultural University Introduced Talent Research Project (XYB201916).

Data availability

The data that has been used is confidential.

References

Barber, T. M., Kabisch, S., Pfeiffer, A. F., & Weickert, M. O. (2020). The health benefits of dietary fibre. *Nutrients, 12*(10), 3209.

Begum, Y. A., & Deka, S. C. (2019). Effect of processing on structural, thermal, and physicochemical properties of dietary fiber of culinary banana bracts. *Journal of Food Processing and Preservation, 43*(12), Article e14256.

Cai, W. D., Zhu, J., Wu, L. X., Qiao, Z. R., Li, L., & Yan, J. K. (2019). Preparation, characterization, rheological and antioxidant properties of ferulic acid-grafted curdlan conjugates. *Food Chemistry, 300*(1), Article 125221.

Chen, B. J., Qiao, Y. J., Wang, X., Zhang, Y., & Fu, L. L. (2023). Extraction, structural characterization, biological functions, and application of rice bran polysaccharides: A review. *Foods, 12*(3), 639.

Chen, Z. G., Zhou, R., Yang, Q., & Zhou, H. X. (2023). The effects of gamma irradiation treatment on starch structure and properties: A review. *International Journal of Food Science & Technology, 58*(9), 4519–4528.

Cheng, T., Liu, C., Hu, Z., Wang, Z., & Guo, Z. (2022). Effects of γ-irradiation on structure and functional properties of pea Fiber. *Foods, 11*(10), 1433.

Chu, J. X., Zhao, H. Z., Lu, Z. X., Lu, F. X., & Bie, X. M. (2019). Improved physicochemical and functional properties of dietary fiber from millet bran fermented by *Bacillus natto*. *Food Chemistry, 294*(1), 79–86.

Hojjati, M., Noshad, M., Sorourian, R., Askari, H., & Feghhi, S. (2023). Effect of gamma irradiation on structure, physicochemical and functional properties of bitter vetch (Vicia ervilia) seeds polysaccharides. *Radiation Physics and Chemistry, 202*, Article 110569.

Hua, M., Lu, J. X., Qu, D., Liu, C., Zhang, L., & Li, S. S. (2019). Structure, physicochemical properties and adsorption function of insoluble dietary fiber from ginseng residue: A potential functional ingredient. *Food Chemistry, 286*, 522–529.

Jia, M. Y., Chen, J. J., Liu, X. Z., Xie, M. Y., Nie, S. P., & Chen, Q. (2019). Structural characteristics and functional properties of soluble dietary fiber from defatted rice bran obtained through trichoderma viride fermentation. *Food Hydrocolloids, 94*, 468–474.

Jiang, C. X., Zeng, B. R., Wei, X. Y., Liu, X. L., Wang, J. T., & Zheng, X. Q. (2024). Improvement of the functional properties of insoluble dietary fiber from corn bran by ultrasonic-microwave synergistic modification. *Ultrasonics Sonochemistry, 104*, Article 106817.

Ju, X., Bowden, M., Brown, E. E., & Zhang, X. (2015). An improved X-ray diffraction method for cellulose crystallinity measurement. *Carbohydrate Polymers, 123*, 476–481.

Khawas, P., & Deka, S. C. (2016). Isolation and characterization of cellulose nanofibers from culinary banana peel using high-intensity ultrasonication combined with chemical treatment. *Carbohydrate Polymers, 137*, 608–616.

Li, X. N., Wang, B. Y., Hu, W. J., Chen, H. G., Sheng, Z. L., & Yang, B. (2022). Effect of γ-irradiation on structure, physicochemical property and bioactivity of soluble dietary fiber in navel orange peel. *Food Chemistry: X, 30*(14), Article 100274.

Liu, Y. L., Zhang, H. B., Yi, C. P., Quan, K., & Lin, B. P. (2020). Chemical composition, structure, physicochemical and functional properties of rice bran dietary fiber modified by cellulase treatment. *Food Chemistry, 342*(16), Article 128352.

Ma, M. M., Mu, T. H., Sun, H. N., Zhang, M., Chen, J. W., & Yan, Z. B. (2015). Optimization of extraction efficiency by shear emulsifying assisted enzymatic hydrolysis and functional properties of dietary fiber from deoiled cumin (*Cuminum cyminum* L.). *Food Chemistry, 179*(15), 270–277.

Ma, Q. Y., Ma, Z. Y., Wang, W. X., Mu, J. L., Liu, Y. Q., & Wang, J. (2022). The effects of enzymatic modification on the functional ingredient-dietary fiber extracted from potato residue. *LWT- Food Science and Technology, 153*, Article 112511.

Morán, J. I., Alvarez, V. A., Cyras, V. P., & Vázquez, A. (2008). Extraction of cellulose and preparation of nanocellulose from sisal fibers. *Cellulose, 15*, 149–159.

Noguerol, A. T., Igual, M. M., & Pagán, M. J. (2022). Developing psyllium fiber gel-based foods: Physicochemical, nutritional, optical and mechanical properties. *Food Hydrocolloids, 122*, Article 107108.

Park, H. Y., Lee, K. W., & Choi, H. D. (2017). Rice bran constituents: Immunomodulatory and therapeutic activities. *Food & Function, 8*(3), 935–943.

Ren, F. Y., Feng, Y. L., Zhang, H. J., & Wang, J. (2021). Effects of modification methods on microstructural and physicochemical characteristics of defatted rice bran dietary fiber. *LWT- Food Science and Technology, 151*, Article 112161.

Singh, J., Metrani, R., Shivanagoudra, S. R., Jayaprakasha, G. K., & Patil, B. S. (2019). Review on bile acids: Effects of the gut microbiome, interactions with dietary fiber, and alterations in the bioaccessibility of bioactive compounds. *Journal of Agricultural and Food Chemistry, 67*(33), 9124–9138.

Song, Y., Su, W., & Mu, Y. C. (2018). Modification of bamboo shoot dietary fiber by extrusion-cellulase technology and its properties. *International Journal of Food Properties, 21*(1), 1219–1232.

Sun, S. F., Yang, J., Wang, D. W., Yang, H. Y., Sun, S. N., & Shi, Z. J. (2021). Enzymatic response of ryegrass cellulose and hemicellulose valorization introduced by sequential alkaline extractions. *Biotechnology for Biofuels, 72*(14).

Sunder, M., Mumbrekar, K. D., & Mazumder, N. (2022). Gamma radiation as a modifier of starch–physicochemical perspective. *Current Research in Food Science, 5*, 141–149.

Swallah, M. S., Fan, H. L., Wang, S. N., Yu, H. S., & Piao, C. H. (2021). Prebiotic impacts of soybean residue (okara) on eubiosis/dysbiosis condition of the gut and the possible effects on liver and kidney functions. *Molecules, 26*(2), 326.

Tang, W., Lin, X., Walayat, N., Liu, J., & Zhao, P. (2024). Dietary fiber modification: Structure, physicochemical properties, bioactivities, and application—a review. *Critical Reviews in Food Science and Nutrition, 64*(22), 7895–7915.

Tian, X. Y., Liu, J. F., Cheng, Z., Wu, N. N., & Tan, B. (2024). Structure, thermal stability, physicochemical and functional characteristics of insoluble dietary fiber obtained from rice bran with steam explosion treatment: Effect of different steam pressure and particle size of rice bran. *Food Research International, 187*, Article 114310.

Tian, Y., Wu, T., Sheng, Y. N., Li, L. N., & Wang, C. Y. (2023). Effects of cavitation-jet technology combined with enzyme treatment on the structure properties and functional properties of OKARA insoluble dietary fiber. *Food Chemistry, 423*, Article 136286.

Wen, Y., Niu, M., Zhang, B., Zhao, S. M., & Xiong, S. B. (2017). Structural characteristics and functional properties of rice bran dietary fiber modified by enzymatic and enzyme-micronization treatments. *LWT- Food Science and Technology, 75*, 344–351.

Wu, C. L., Teng, F., McClements, D. J., Zhang, S., Li, Y., & Wang, Z. J. (2020). Effect of cavitation jet processing on the physicochemical properties and structural characteristics of okara dietary fiber. *Food Research International, 134*, Article 109251.

Xu, Y. J., Zhang, C. C., Liao, Z. H., Li, Z. J., Xu, X. M., Sui, Z. Q., & Corke, H. (2022). Optimization of soluble dietary fiber extraction from hulless barley grass. *Cereal Chemistry, 99*(3), 482–492.

Yang, X., Dai, J., Zhong, Y., Wei, X. L., Wu, M. X., & Zhang, Y. X. (2021). Characterization of insoluble dietary fiber from three food sources and their potential hypoglycemic and hypolipidemic effects. *Food & Function, 12*(14), 6576–6587.

Yang, Z. B., Zeng, Y. D., Hu, Y. D., Zhou, T. T., Li, J. M., & He, L. L. (2023). Comparison of chemical property and in vitro digestion behavior of polysaccharides from

auricularia polytricha mycelium and fruit body. *Food Chemistry: X, 17*, Article 100570.
Yegin, S., Kopec, A., Kitts, D. D., & Zawistowski, J. (2020). Dietary fiber: A functional food ingredient with physiological benefits. *Dietary Sugar, (Salt and Fat in Human Health)*.
Zhang, L., Wu, T., Zhang, Y. L., Chen, Y. J., Ge, X. F., & Sui, W. J. (2023). Release of bound polyphenols from wheat bran soluble dietary fiber during simulated gastrointestinal digestion and colonic fermentation in vitro[J]. *Food Chemistry, 402*, Article 134111.
Zhang, S., Xu, X., Cao, X., & Liu, T. T. (2023). The structural characteristics of dietary fibers from tremella fuciformis and their hypolipidemic effects in mice. *Food Science and Human Wellness, 12*(2), 503–511.
Zhang, Y., Qi, J. R., Zeng, W. Q., Huang, Y. X., & Yang, X. Q. (2020). Properties of dietary fiber from citrus obtained through alkaline hydrogen peroxide treatment and homogenization treatment. *Food Chemistry, 311*, Article 125873 (C).
Zheng, Y. J., Xu, B. F., Shi, P. Q., Tian, H. L., Li, Y., & Wang, X. Y. (2022). The influences of acetylation, hydroxypropylation, enzymatic hydrolysis and crosslinking on improved adsorption capacities and in vitro hypoglycemic properties of millet bran dietary fiber. *Food Chemistry, 368*(30), Article 130883.
Zhu, L., Yu, B., Chen, H., Yu, J., Yan, H., & Luo, Y. H. (2022). Comparisons of the micronization, steam explosion, and gamma irradiation treatment on chemical composition, structure, physicochemical properties, and in vitro digestibility of dietary fiber from soybean hulls. *Food Chemistry, 366*, Article 130618.